Available online at www.sciencedirect.com
ScienceDirect
Trans. Nonferrous Met. Soc. China 28(2018) 819−828
Transactions of Nonferrous Metals Society of China
www.tnmsc.cn

Measurement of phase equilibria in Ti−Ni−Sn system

Meng WANG, Hua-shan LIU, Ge-mei CAI, Zhan-peng JIN

School of Materials Science and Engineering, Central South University, Changsha 410083, China

Received 22 November 2016; accepted 7 July 2017

Abstract: Phase relations of the Ti−Ni−Sn ternary system were investigated via alloy sampling assisted with X-ray diffractometry (XRD) and electron probe micro-analysis (EPMA). A new binary phase with composition of $TiSn_4$ (molar fraction, %) was detected at 508 K. In addition, a supplementary phase $(Ti_{1-x-y}Ni_xSn_y)Ni_3$ (τ, $AuCu_3$-type) was observed at 873 and 973 K. According to the characterised microscopic structure in various annealed alloys, four ternary phases were detected in Ti−Ni−Sn ternary system: TiNiSn, $TiNi_2Sn$, Ti_2Ni_2Sn and $(Ti_{1-x-y}Ni_xSn_y)Ni_3$. Additionally, isothermal sections of Ti−Ni−Sn ternary system at 508, 873 and 973 K were constructed. By comparing three isothermal sections, a peri-eutectic reaction, L+$TiNi_2Sn$→Ni_3Sn_4+TiNiSn, was deduced, which occurs at a temperature between 873 and 973 K. Furthermore, the solubility of Sn in TiNi and Ni in Ti_5Sn_3 was detected.
Key words: isothermal section; Ti−Ni−Sn system; phase equilibria

1 Introduction

Ti−Ni based alloys belong to one of the most important shape memory alloys (SMAs). They involve three types of martensitic transformations, which are responsible for their excellent shape memory effect along with pseudo-elasticity [1]. Methods, including thermo-mechanical treatments and/or alloying, have been investigated to improve the shape memory (SM) properties of these alloys for industrial and medical applications.

Element addition to the Ti−Ni alloys exerts significant effect on martensitic transformation and thus on mechanical behaviour. Recently, Sn addition to the Ti−Ni alloys has attracted increasing attention [2−7]. It has been reported that Sn can bring about one-staged $B19'$−$B2$ transformation upon heating [2,3] and two-staged $B2$−R−$B19'$ martensitic transformation during cooling [3,4]. Also, the starting temperature (T_R) for $B2$−R transformation decreases with increase of Sn content [6]. To better comprehend the role of Sn in Ti−Ni SMAs, knowledge of phase equilibrium in the Ti−Ni−Sn system is of great significance importance.

2 Phase relationship of Ti−Ni−Sn system in literatures

2.1 Binary system

Phase diagram of the Ti−Ni binary system has been studied experimentally and thermodynamically [8−18]. Most of the experiments on the Ti−Ni binary system are related to martensitic transformation [8,9]. For phase diagram studies, KAUFMAN and NESOR [10] calculated this system firstly. They regarded all the intermediate compounds as line compounds. Subsequently, MURRAY [11] assessed this system after considering literature data up to 1985. LIANG and JIN [12] used the sub-regular solution model to reevaluate the terminal solid solutions ((α-Ti), (β-Ti), (Ni)), and treated the Ti_2Ni and $TiNi_3$ as line compounds. More recently, JIA et al [13] investigated the solubility range of the $TiNi_3$ phase. Following this, BELLEN et al [14], TANG et al [15] and DEKEYZER et al [16] used single Gibbs energy to describe the order and disordered phase in the TiNi phase. Then, TOKUNAGA et al [17], SANTHY and KUMAR [18] and POVODEN-KARADENIZ et al [19] optimised this system. Recently, POVODEN-KARADENIZ et al [19] provided new

Foundation item: Project (2016YFB0701404) supported by the National Key Research and Development Program of China; Project (51171210) supported by the National Natural Science Foundation of China; Project (2014CB6644002) supported by the National Basic Research Program of China
Corresponding author: Hua-shan LIU; Tel: +86-731-88879341; Fax: +86-731-88876692; E-mail: hsliu@csu.edu.cn
DOI: 10.1016/S1003-6326(18)64715-6

thermodynamic data about the D024-ordered $TiNi_3$ phase and two metastable Ti_3Ni_4 and Ti_2Ni_3 phases. According to POVODEN-KARADENIZ et al [19], four stable compounds, i.e., $TiNi_3$, Ti_2Ni, $B19'$ and TiNi exist in the Ti−Ni system.

As for the Ti−Sn system, FINLAY et al [20], McQUILLAN et al [21], and GLAZOVA and KURNAKOV [22] studied the Ti-rich part of Ti−Sn system. BONDAR et al [23] and EREMENKO and VELIKANOVA [24] studied the phase transformation of the $Ti_{81.5}Sn_{18.5}$ alloy and the Sn-rich part by DTA. In addition, KUPER et al [25] found a new intermetallic phase Ti_2Sn_3 with a composition of about 60% Sn (molar fraction). Recently, YIN et al [26] performed DTA experiments at Sn-rich side and used these results in the assessment. It is accepted that the Ti−Sn system contains five stable intermetallic compounds: Ti_3Sn, Ti_2Sn, Ti_5Sn_3, Ti_6Sn_5 and Ti_2Sn_3.

Most of the experiments in the Ni−Sn system date back to the first half of the 20th Century [27,28]. Recently, LIU et al [29] assessed this binary system, which included the intermediate phases Ni_3Sn_LT, Ni_3Sn_HT, Ni_3Sn_2_LT, Ni_3Sn_2_HT and Ni_3Sn_4.

2.2 Ternary system

There have been reports about phase equilibria in the Ti−Ni−Sn ternary system. Phase relations of the Ti−Ni−Sn ternary system at 770 K were measured by STADNYK and SKOLOZDRA [30] firstly. Later, isothermal sections at 1073 K [31] and 1223 K [32] have been subsequently determined. The existence of the Ti_5NiSn_3 compound was reported by SCHUSTER et al [33], who believed that this compound was a substitutional solution of Ti_5Sn_3 containing Ni, rather than a ternary phase. Meanwhile, BERCHE et al [34] reported that Sn substitutes Ni in equiatomic TiNi alloy, forming a pseudo-binary system. More recently, a supplementary phase $(Ti_{1-x-y}Ni_xSn_y)Ni_3$ (τ, $AuCu_3$-type) was reported by GÜRTH et al [32]. So far, four ternary phases have been detected in the Ti−Ni−Sn ternary system, namely, TiNiSn, $TiNi_2Sn$, Ti_2Ni_2Sn and $(Ti_{1-x-y}Ni_xSn_y)Ni_3$.

However, stability of the compound Ti_2Ni_2Sn in the Ti−Ni−Sn ternary system at 770 K is not so clear. According to ROMAKA et al [31], Ti_2Ni_2Sn was stable between 673 K and 1073 K, but it was not observed in the ternary phase diagram of the Ti−Ni−Sn system at 770 K [30]. This work tends to measure phase equilibria in the Ti−Ni−Sn ternary system at 508, 873 and 973 K.

3 Experimental

Alloy sampling was adopted to experimentally study phase relations of the Ti−Ni−Sn system at 508, 873 and 973 K. More than 40 alloys have been prepared. Raw materials of high purity (99.99% Ti, 99.99% Ni, and 99.99% Sn, mass fraction) were used to prepare the experimental alloys. The mass of each sample was limited to be about 8 g. Pre-determined amount of each raw material was weighted with analytical balance. Then, the weighted raw materials were mixed and melted by arc-melting in a water-cooled copper crucible under high purity argon atmosphere (with Ti getter). To ensure the homogeneity, all alloys were re-melted at least four times. After direct arc melting, all raw materials became button alloys and were weighted again. The mass losses were found to be less than 1% of the total mass. Subsequently, the button alloys were cut into four parts. Each part was respectively annealed at 508 K for 180 d, 873 K for 100 d, and 973 K for 90 d in the evacuated quartz tubes, and followed by quenching in ice water.

Constituent phases in annealed samples were studied by electron probe microanalysis (EPMA) (JXA−8800R, JEOL, Japan) equipped with OXFORD INCA 500 wavelength dispersive X-ray spectrometer (WDS). Standard deviations of the measured concentration are ±0.6% (molar fraction). The total content of Ti, Ni and Sn in each phase is in the range of 97%−103% (molar fraction), indicating that reaction between alloy and silica capsules can be neglected. X-ray diffraction (XRD) was also performed to the same annealed alloys using a Cu K_α radiation on a Rigaku D-max/2550VB+ X-ray diffractometer at 40 kV and 30 mA. By comparing the XRD patterns of the samples with the powder diffraction database (PDF-4+2012) of the International Center for Diffraction Data (ICDD), the phase compositions of each sample were determined.

4 Results

4.1 Phase equilibrium at 508 K

More than 40 samples covering the entire composition range were employed to determine phase relations in the Ti−Ni−Sn ternary system at 508 K. The constituent phases in the annealed alloys and corresponding equilibria are summarized in Table 1.

Microstructure of the Ti-rich Alloy A1 annealed at 508 K is illustrated in Fig. 1(a). According to EPMA analysis, A1 is composed of Ti_3Sn, solution (Ti) and Ti_2Ni. As shown in Fig. 1(b), X-ray diffraction for A1 discloses existence of solution (Ti), Ti_2Ni, and Ti_3Sn. That is to say, A1 locates in the three-phase region of Ti_3Sn+Ti_2Ni+Ti. It is also worth nothing that about 10% (molar fraction) Sn dissolves in (Ti) according to EPMA−WDS analysis.

Figure 2(a) shows back-scattered electron (BSE) image of the Sn-rich Alloy A5 after annealing at 508 K, where three phases could be observed. According to

Table 1 Constituent phases in annealed Ti−Ni−Sn alloys at 508 K

Alloy	Composition of alloy (molar fraction)/%	Phase equilibrium			Composition of phase (molar fraction)/%								
		Phase 1	Phase 2	Phase 3	Phase 1			Phase 2			Phase 3		
					Ti	Ni	Sn	Ti	Ni	Sn	Ti	Ni	Sn
A1	Ti80Ni10Sn10	Ti_2Ni	Ti	Ti_3Sn	67.99	29.84	2.17	84.17	5.73	10.1	77.38	3.75	18.87
A2	Ti70Ni10Sn20	Ti_2Ni	TiNi	Ti_3Sn	65.97	31.98	2.05	53.64	43.85	2.51	74.24	1.19	24.57
A3	Ti60Ni10Sn30	TiNi	Ti_3Sn	Ti_5NiSn_3	52.84	45.54	1.62	74.15	2.05	23.80	58.61	9.99	31.40
A4	Ti50Ni40Sn10	Ti_5NiSn_3	TiNi	−	57.19	11.17	31.64	49.45	47.58	2.97	−	−	−
A5	Ti40Ni20Sn40	$TiSn_4$	Ti_6Sn_5	TiNiSn	19.47	0.95	79.58	52.53	4.40	43.07	32.05	35.08	32.87
A6	Ti40Ni30Sn30	$TiNi_2Sn$	Ti_5NiSn_3	Ti_6Sn_5	28.02	46.53	25.45	56.45	8.77	34.78	52.20	5.06	42.74
A7	Ti40Ni40Sn20	$TiNi_2Sn$	Ti_5NiSn_3	TiNi	28.75	46.72	24.53	55.90	11.42	32.68	47.09	47.83	5.08
A8	Ti30Ni30Sn40	TiNiSn	Sn	−	32.54	35.00	32.46	5.45	4.71	89.84	−	−	−
A9	Ti30Ni60Sn10	$TiNi_3$	$TiNi_2Sn$	−	26.44	73.46	0.10	27.51	50.65	21.84	−	−	−
A10	Ti20Ni20Sn60	$TiSn_4$	TiNiSn	Sn	16.97	0.23	82.8	32.71	35.19	32.10	0.61	1.08	98.31
A11	Ti20Ni50Sn30	$TiNi_2Sn$	Ni_3Sn_2	Ni_3Sn_4	25.43	49.90	24.67	1.32	55.39	43.29	0.37	43.68	55.95
A12	Ti10Ni70Sn20	Ni_3Sn_2	$TiNi_3$	−	1.68	62.58	35.74	19.62	74.41	5.97	−	−	−
A13	Ti10Ni80Sn10	Ni_3Sn	$TiNi_3$	Ni	0.93	74.35	24.72	15.94	75.59	8.47	8.01	80.41	11.58
A14	Ti10Ni40Sn50	Ni_3Sn_4	TiNiSn	−	0.11	42.29	57.60	32.11	36.57	31.32	−	−	−
A15	Ti10Ni60Sn30	$TiNi_2Sn$	Ni_3Sn_2	−	23.51	52.45	24.04	1.32	63.33	35.35	−	−	−
A16	Ti24Ni28Sn48	Ni_3Sn_4	TiNiSn	Sn	0.05	42.00	57.95	32.01	33.94	34.05	0.05	0.95	99.00
A17	Ti25Ni50Sn25	Ni_3Sn_4	$TiNi_2Sn$	−	0.16	42.27	57.57	26.66	47.00	26.34	−	−	−
A18	Ti65Ni5Sn30	Ti_3Sn	Ti_2Sn	Ti_5NiSn_3	74.74	1.70	23.56	68.35	2.62	29.03	57.96	10.72	31.32
A19	Ti35Ni35Sn30	$TiNi_2Sn$	Ti_6Sn_5	−	28.48	44.86	26.66	55.10	4.53	40.37	−	−	−

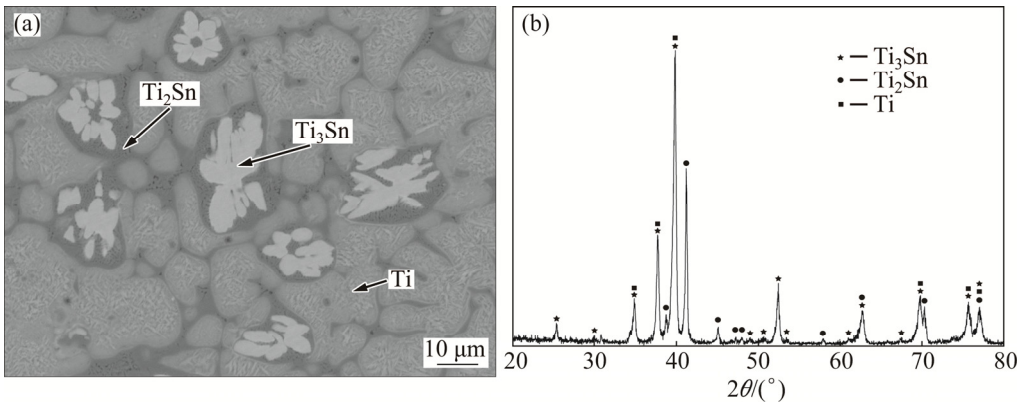

Fig. 1 Constituent phases in Alloy A1 annealed at 508 K: (a) BSE image; (b) Corresponding XRD patterns

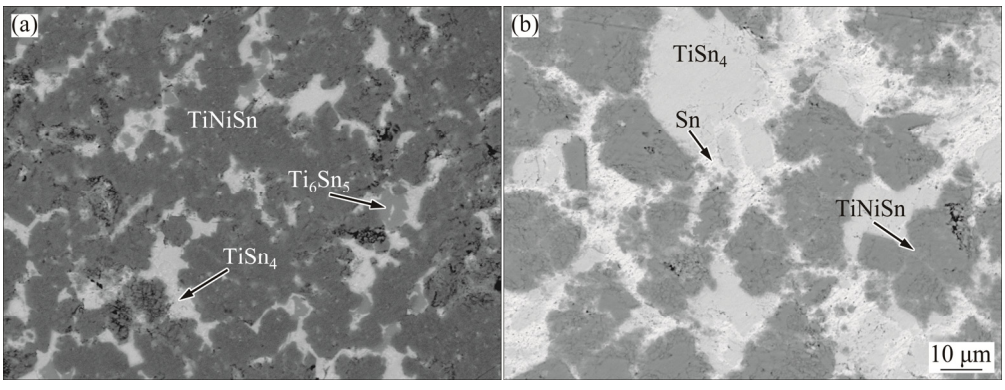

Fig. 2 BSE images of ternary alloys annealed at 508 K: (a) Alloy A5; (b) Alloy A10

EPMA−WDS, the black phase is TiNiSn, the gray is Ti_6Sn_5 and the bright one is a phase with composition of $Ti_{19.47}Ni_{0.95}Sn_{79.58}$. BSE image of Alloy A10 is shown in Fig. 2(b), which contains the bright phase Sn, the dark gray TiNiSn and an unknown phase whose composition is $Ti_{16.97}Ni_{0.23}Sn_{82.8}$, close to that in A5. It is guessed that $Ti_{19.47}Ni_{0.95}Sn_{79.58}$ in A5 and $Ti_{16.97}Ni_{0.23}Sn_{82.8}$ in A10 are the same phase, and both are of composition close to the formula $TiSn_4$. So, they are temporarily called the $TiSn_4$ phase here. In order to confirm the existence of $TiSn_4$, X-ray diffraction was carried out for alloys A5 and A10. Except for the peaks indexed to Ti_6Sn_5, TiNiSn and Sn, some peaks remained unidentified in Fig. 3(a) and in Fig. 3(b) show correspondingly similar angles and relative intensity. These unindexed peaks should belong to the unknown phase $TiSn_4$. Further work is necessary to determine the crystal structure and standard PDF of $TiSn_4$.

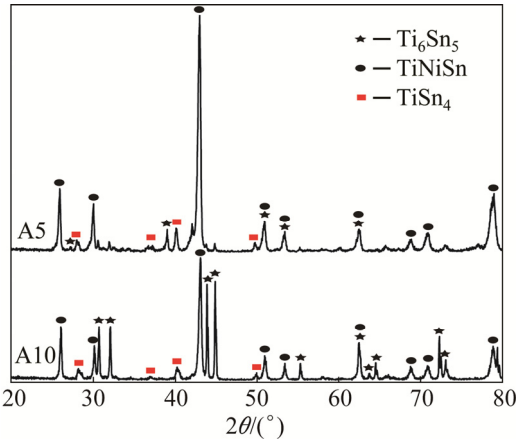

Fig. 3 XRD patterns of A5 and A10 ternary alloys annealed at 508 K

As seen in Fig. 4, the dark-gray $TiNi_2Sn$, gray Ti_5NiSn_3, and bright Ti_6Sn_5 in Alloy A6, and the dark black TiNi, gray $TiNi_2Sn$, and bright Ti_5NiSn_3 in Alloy A7 could be easily distinguished via EPMA. This means that two three-phase regions are determined, i.e., $TiNi_2Sn$+Ti_5NiSn_3+Ti_6Sn_5 and $TiNi_2Sn$+Ti_5NiSn_3+TiNi.

Figure 5 illustrates that constituent phases Ti_3Sn, Ti_2Sn and Ti_5NiSn_3 coexist in A18, indicating that there exists a three-phase region: Ti_2Sn+Ti_3Sn+Ti_5NiSn_3.

Based on the experimental results of this work and the relevant binary systems, isothermal section of the Ti−Ni−Sn ternary system at 508 K is constructed (Fig. 6), which consists of 19 three-phase and 34 two-phase regions. The single-phase region $TiNi_3$ extends along the iso-concentration of Ni, implying that Sn substitutes for Ti in $TiNi_3$. The solubility of Sn in $TiNi_3$ is found to be 6.5% (molar fraction). And binary phases TiNi and Ti_5Sn_3 show remarkable ternary solubility, e.g., the solubility of Sn in TiNi can be up to 5.08% and the

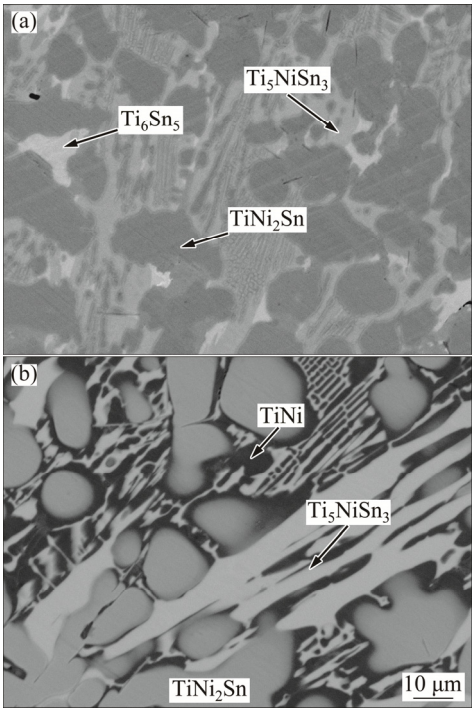

Fig. 4 BSE images of annealed alloys at 508 K: (a) Alloy A6; (b) Alloy A7

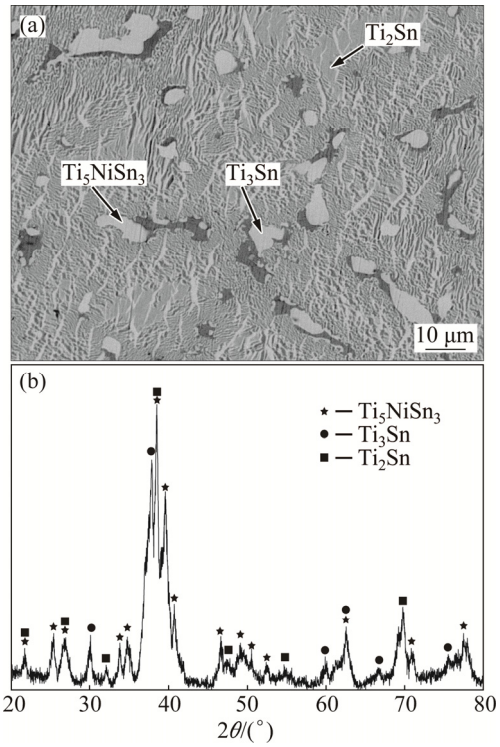

Fig. 5 Constituent phases in Alloy A18: (a) BSE image; (b) XRD pattern

solubility of Ni in Ti_5Sn_3 can up to 11.42%. It is worth noting that the three-phase equilibrium $TiSn_4$+Ti_6Sn_5+Ti_2Sn_3 was deduced based on the Sn-rich part of the Ti−Sn binary system and the adjacent three-phase region TiNiSn+Ti_6Sn_5+$TiSn_4$.

4.2 Phase equilibrium at 873 K

To determine the isothermal section at 873 K, 18 samples were synthesized. The detected equilibrium phases in various samples are listed in Table 2.

Figure 7(a) exhibits BSE image of Alloy B5, where the gray Ti_2Ni_2Sn, gray TiNiSn, and bright Ti_5NiSn_3 are detected. Ti_2Ni_2Sn was also observed in Alloy B6 (Fig. 7(b)) which shows a three-phase equilibrium: Ti_2Ni_2Sn+ $TiNi_2Sn$+TiNi.

Microstructure of Alloy B8 is revealed in Fig. 8(a). According to BSE and the EPMA analysis, the bright $TiNi_2Sn$ is the primary crystal, which is surrounded by the gray eutectic structure (TiNi and $TiNi_3$). To confirm this three-phase region, X-ray diffraction analysis was

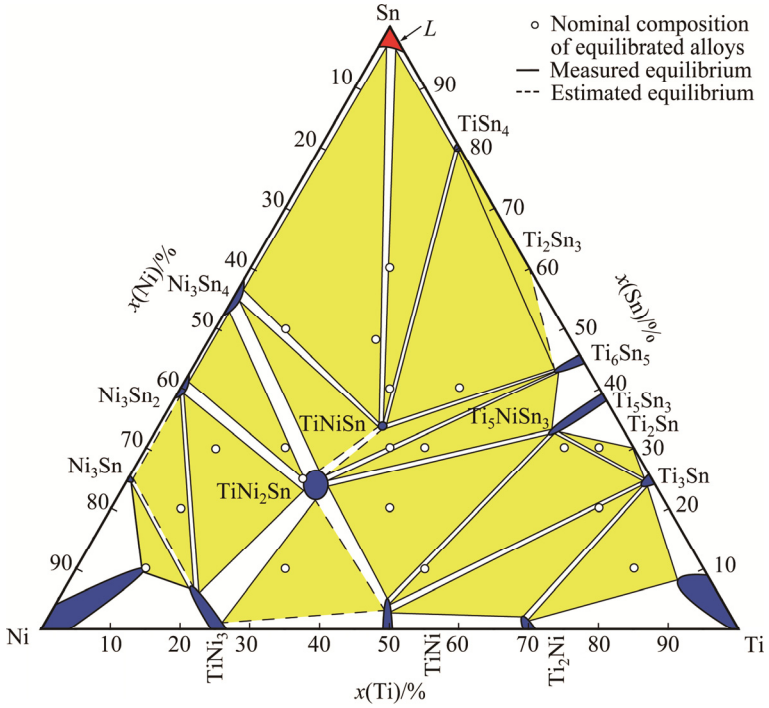

Fig. 6 Isothermal section of Ti−Ni−Sn ternary system at 508 K

Table 2 Constituent phases in annealed Ti−Ni−Sn alloys at 873 K

Alloy	Composition of alloy (molar fraction)/%	Phase equilibrium			Composition of phase (molar fraction)/%								
		Phase 1	Phase 2	Phase 3	Phase 1			Phase 2			Phase 3		
					Ti	Ni	Sn	Ti	Ni	Sn	Ti	Ni	Sn
B1	Ti80Ni10Sn10	Ti_2Ni	Ti	−	67.96	30.65	1.39	86.09	2.01	11.90	−	−	−
B2	Ti70Ni10Sn20	Ti_2Ni	Ti	Ti_3Sn	69.08	29.38	1.54	86.62	1.52	11.86	79.65	0.40	19.95
B3	Ti60Ni10Sn30	Ti_3Sn	TiNi	Ti_5NiSn_3	75.50	0.82	23.68	58.10	32.27	9.63	57.27	10.25	32.48
B4	Ti40Ni20Sn40	TiNiSn	Ti_6Sn_5	Ti_2Sn_3	33.85	33.21	32.94	54.61	0.17	45.22	40.26	0.51	59.23
B5	Ti40Ni30Sn30	Ti_2Ni_2Sn	TiNiSn	Ti_5NiSn_3	40.34	36.11	23.55	36.29	33.15	30.56	55.41	11.11	33.48
B6	Ti40Ni40Sn20	TiNi	Ti_2Ni_2Sn	$TiNi_2Sn$	46.54	45.59	7.87	42.79	39.09	18.12	29.46	46.47	24.07
B7	Ti30Ni30Sn40	TiNiSn	Liquid	−	33.92	33.42	32.66	0.67	0.60	98.73	−	−	−
B8	Ti30Ni60Sn10	TiNi	$TiNi_3$	$TiNi_2Sn$	45.53	52.93	1.54	25.65	74.23	0.12	26.7	52.15	21.15
B9	Ti20Ni20Sn60	TiNiSn	Ni_3Sn_4	Liquid	34.22	32.69	33.09	0.19	38.13	61.68	0.30	1.42	98.28
B10	Ti25Ni45Sn30	$TiNi_2Sn$	Ni_3Sn_4	TiNiSn	24.75	50.53	24.72	0.41	46.93	52.66	32.25	35.13	32.62
B11	Ti10Ni70Sn20	$TiNi_3$	Ni_3Sn_2	−	18.67	75.14	6.19	0.46	62.06	37.48	−	−	−
B12	Ti10Ni80Sn10	τ	Ni_3Sn	$TiNi_3$	10.73	78.42	10.85	0.75	75.10	24.15	14.37	79.57	6.06
B13	Ti20Ni30Sn50	TiNiSn	Ni_3Sn_4	Liquid	34.02	33.29	32.69	0.01	42.16	57.83	−	1.61	98.39
B14	Ti10Ni40Sn50	TiNiSn	Ni_3Sn_4	−	33.72	34.24	32.04	−	44.97	55.03	−	−	−
B15	Ti25Ni50Sn25	$TiNi_2Sn$	−	−	24.98	49.41	25.61	−	−	−	−	−	−
B16	Ti65Ni5Sn30	Ti_3Sn	Ti_5NiSn_3	−	75.32	0.41	24.27	59.39	8.66	31.95	−	−	−
B17	Ti35Ni35Sn30	TiNiSn	Ti_5NiSn_3	Ti_6Sn_5	34.43	32.01	33.56	55.09	8.10	36.81	55.06	0.72	44.22
B18	Ti10Ni60Sn30	$TiNi_2Sn$	Ni_3Sn_2	$TiNi_3$	23.00	51.73	25.27	0.65	61.64	37.71	20.67	74.31	5.02

employed, as shown in Fig. 8(b). Thus, the three-phase equilibrium $TiNi_2Sn+TiNi_3+TiNi$ is determined.

According to Fig. 9, equilibria $TiNi+Ti_3Sn+Ti_5NiSn_3$ and $TiNi_2Sn+Ni_3Sn_2+TiNi_3$ are determined.

As seen from Figs. 10(a) and (b), constituent phases Ni_3Sn, Ni and τ coexist in B12 at 873 K.

Microstructure of Alloy B13 is demonstrated in Fig. 11, where the dark gray TiNiSn and gray Ni_3Sn_4 can be easily determined. The bright area is Sn-rich and of composition of $Ni_{1.6}Sn_{98.4}$. In light of the Ni−Sn and

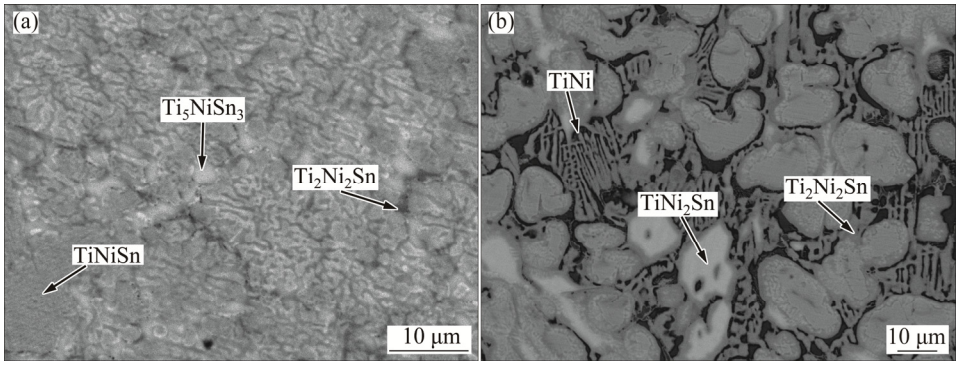

Fig. 7 BSE images of ternary alloys annealed at 873 K: (a) Alloy B5; (b) Alloy B6

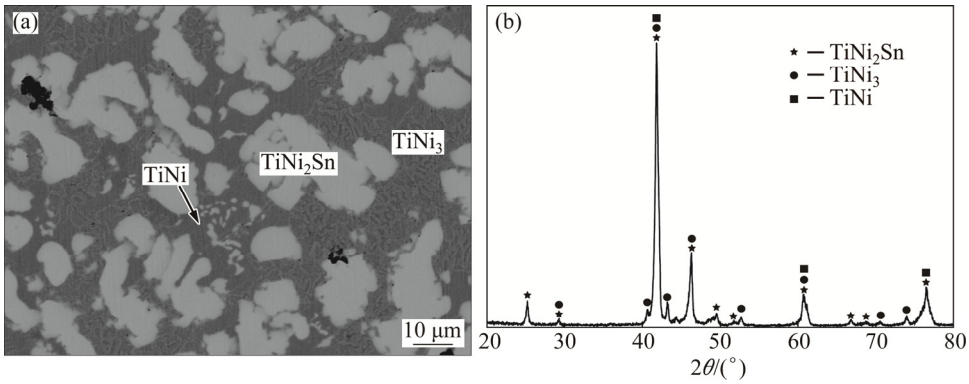

Fig. 8 Constituent phases in Alloy B8 annealed at 873 K: (a) BSE image; (b) XRD pattern

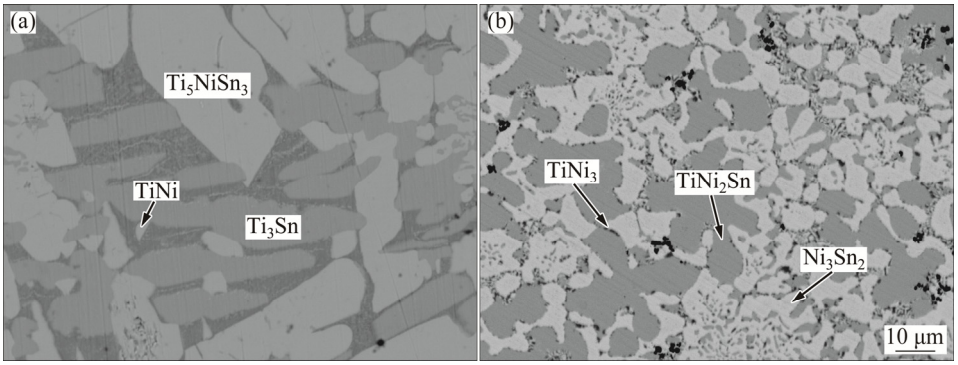

Fig. 9 BSE images of ternary alloys annealed at 873 K: (a) Alloy B3; (b) Alloy B18

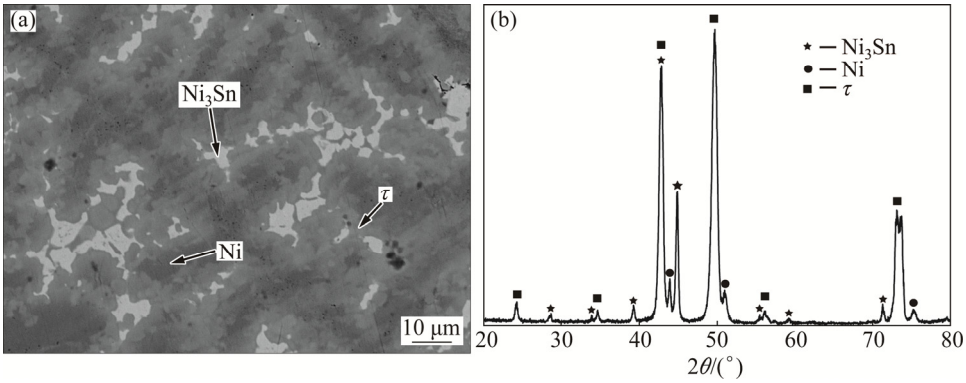

Fig. 10 Constituent phases in Alloy B12 annealed at 873 K: (a) BSE image; (b) XRD pattern

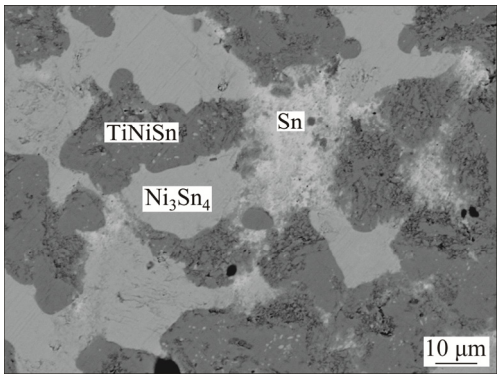

Fig. 11 BSE image of Alloy B13 ternary alloys annealed at 873 K

Ti−Sn binary systems, the bright area in Fig. 11 must be the liquid phase which exists stably during annealing at 873 K. Thus, the actual equilibrium in Alloy B13 should be TiNiSn+Ni_3Sn_4+Liquid.

So far, isothermal section of the Ti−Ni−Sn ternary system at 873 K can be established, as described in Fig. 12, where 20 three-phase and 36 two-phase regions are identified. In addition, ternary solubility in binary compounds is remarkable, e.g., Sn in TiNi can be up to 7.87%, and Ni in Ti_5Sn_3 can be up to 11.11%, respectively.

4.3 Phase equilibrium at 973 K

More than 40 alloy samples were prepared for determining the isothermal section of the Ti−Ni−Sn ternary system at 973 K. Phase equilibria have been detected, as summarized in Table 3.

In light of Fig. 13, constituent phases in Alloy C8 include (Sn) and TiNiSn. Easy to be understood, (Sn) should exist as liquid when Alloy C5 was annealed at 973 K. This means that C8 locates in the two-phase field of Liquid+TiNiSn at 973 K.

BSE image of Alloy C15 is presented in Fig. 14. With EPMA−WDS analysis, it can be known that C15 involves the dark gray $TiNi_2Sn$, the gray Ni_3Sn_4 and the bright (Sn) which is actually liquid. Therefore, the three-phase region Liquid+$TiNi_2Sn$+Ni_3Sn_4 can be identified.

So far, isothermal section of the Ti−Ni−Sn ternary system at 973 K can be constructed, as demonstrated in Fig. 15, where 20 three-phase regions and 36 two-phase regions are identified. By the way, ternary solubility in binary compounds is remarkable, e.g., the solubility of Sn in TiNi can be up to 4.60%, and that of Ni in Ti_5Sn_3 can be up to 12.24%, respectively.

5 Discussion

By recalling Figs. 6 and 12, a preliminary comparison of the phase relation can be made at 508 and 873 K. The ternary phase Ti_2Ni_2Sn that is observed at 873 K, firstly disappears at 508 K. This agrees with ROMAKA et al [31], that Ti_2Ni_2Sn is stable from 673 to 1073 K. Secondly, the new binary phase $TiSn_4$, is stable at 508 K before disappearing at 873 K. In this work, the alloys were annealed at 508 K for 180 d, ensuring full equilibrium. The $TiSn_4$ phase in the BSE images is large and uniform.

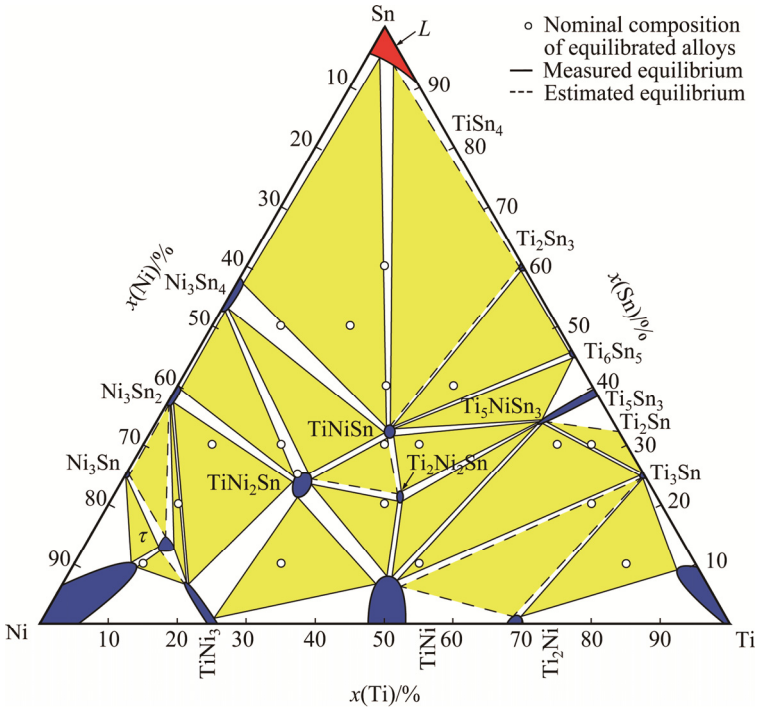

Fig. 12 Isothermal section of Ti−Ni−Sn ternary system at 873 K

Table 3 Constituent phases in annealed Ti−Ni−Sn alloys at 973 K

Alloy	Composition of alloy (molar fraction/%)	Phase equilibrium			Composition of phase (molar fraction)/%								
		Phase 1	Phase 2	Phase 3	Phase 1			Phase 2			Phase 3		
					Ti	Ni	Sn	Ti	Ni	Sn	Ti	Ni	Sn
C1	Ti80Ni10Sn10	Ti_2Ni	Ti	Ti_3Sn	71.61	25.78	2.61	86.45	0.62	12.93	78.96	0.5	20.54
C2	Ti70Ni10Sn20	TiNi	Ti_3Sn	−	53.9	42.82	3.28	74.65	0.67	24.68	−	−	−
C3	Ti60Ni10Sn30	Ti_5NiSn_3	Ti_3Sn	−	55.09	8.88	36.03	72.08	0.89	27.03	−	−	−
C4	Ti50Ni40Sn10	Ti_5NiSn_3	Ti_2Ni_2Sn	TiNi	56.33	12.24	31.43	46.14	38.31	15.55	51.59	47.45	0.96
C5	Ti40Ni20Sn40	Ti_2Sn_3	Ti_6Sn_5	TiNiSn	37.42	1.8	60.78	51.59	2	46.41	31.67	33.11	35.22
C6	Ti40Ni30Sn30	Ti_5NiSn_3	TiNiSn	−	55.15	10.03	34.82	34.39	36.17	29.44	−	−	−
C7	Ti40Ni40Sn20	Ti_2Ni_2Sn	$TiNi_2Sn$	TiNiSn	40.6	39.36	20.04	29.23	46	24.77	34.46	34.08	31.46
C8	Ti30Ni30Sn40	TiNiSn	Liquid	−	33.88	32.49	33.63	0.45	0.93	98.62	−	−	−
C9	Ti30Ni60Sn10	$TiNi_3$	TiNi	$TiNi_2Sn$	26.61	73.28	0.11	44.46	50.94	4.6	29.48	49.34	21.18
C10	Ti20Ni20Sn60	TiNiSn	Liquid	−	34.07	32.26	33.67	0.03	0.27	99.7	−	−	−
C11	Ti20Ni50Sn30	Ni_3Sn_4	Ni_3Sn_2	$TiNi_2Sn$	0.37	45.71	53.92	0.31	54.13	45.56	24.55	49.12	26.33
C12	Ti10Ni70Sn20	τ	Ni_3Sn_2	−	16.08	74.64	9.28	1.9	62.85	35.25	−	−	−
C13	Ti10Ni80Sn10	Ni	τ	Ni_3Sn	3.58	91.59	4.83	11.8	77.71	10.49	0.54	75.44	24.02
C14	Ti10Ni60Sn30	Ni_3Sn_2	$TiNi_2Sn$	$TiNi_3$	0.29	60.31	39.4	22.05	51.8	26.15	22.24	73.18	4.58
C15	Ti20Ni30Sn50	$TiNi_2Sn$	Ni_3Sn_4	Liquid	25.64	48	26.36	0	42.86	57.14	0.01	4.14	95.85
C16	Ti25Ni50Sn25	$TiNi_2Sn$	−	−	25.99	48.43	25.58	−	−	−	−	−	−
C17	Ti65Ni5Sn30	Ti_5NiSn_3	Ti_3Sn	−	55.31	9.99	34.7	71.77	1.33	26.9	−	−	−
C18	Ti35Ni35Sn30	TiNiSn	$TiNi_2Sn$	−	31.44	34.26	34.3	26.86	45.64	27.5	−	−	−

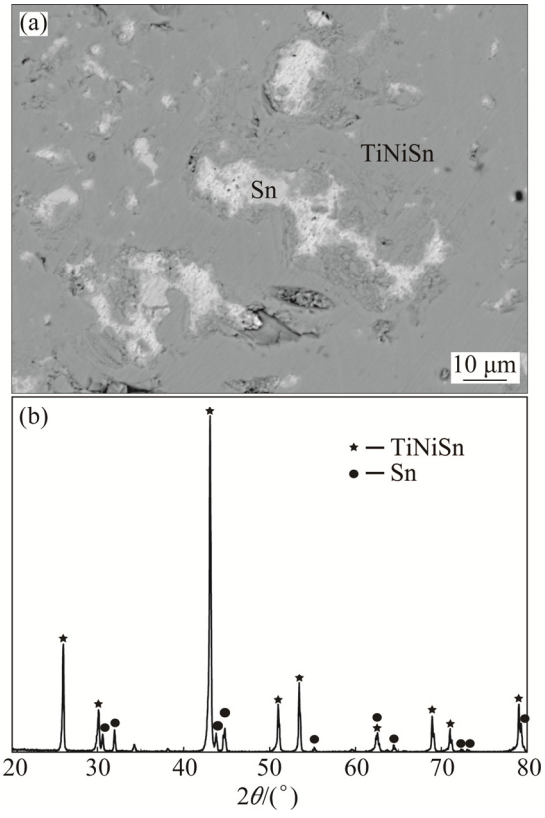

Fig. 13 Constituent phase in Alloy C8 annealed at 973 K: (a) BSE image; (b) XRD pattern

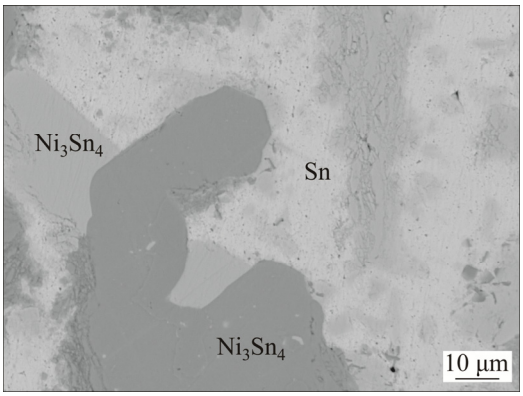

Fig. 14 BSE image of Alloy C15 ternary alloys annealed at 973 K

As seen in Figs. 12 and 15, a notable difference can be manifested between the isothermal sections at 873 K, and 973 K. When the temperature decreases from 973 to 873 K, the three-phase regions, Sn+Ni_3Sn_4+$TiNi_2Sn$ and Sn+TiNiSn+$TiNi_2Sn$, transform into two other three-phase regions, Sn+Ni_3Sn_4+TiNiSn and Ni_3Sn_4+$TiNi_2Sn$+TiNiSn. It can be inferred that a peri-eutectic reaction L+$TiNi_2Sn$→Ni_3Sn_4+TiNiSn between 873 and 973 K must occur. Recently, BERCHE et al [34] thermodynamically assessed the Ti−Ni−Sn ternary system. By adopting thermodynamic parameters from

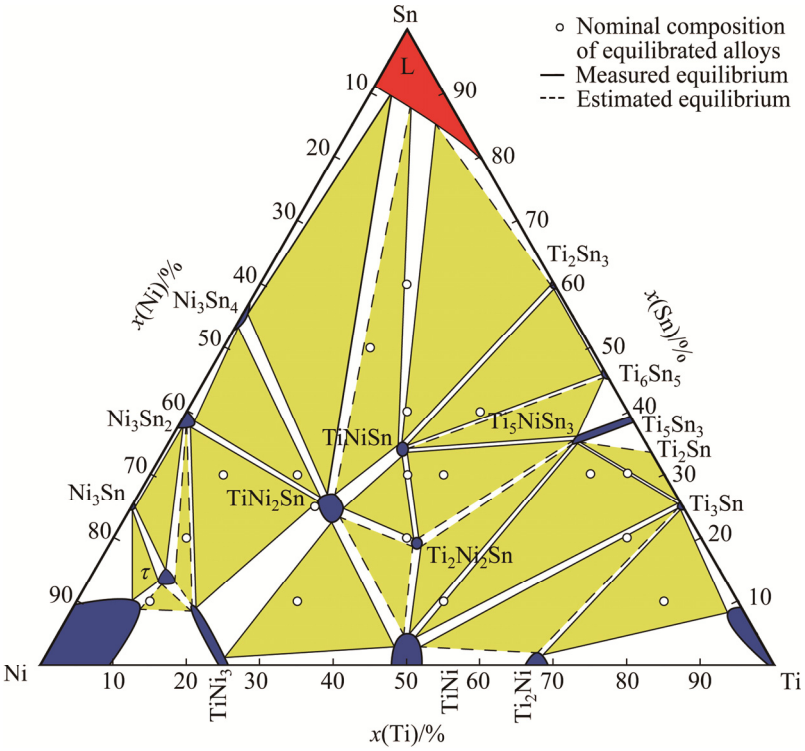

Fig. 15 Isothermal section of the Ti−Ni−Sn ternary system at 973 K

BERCHE et al [34], peri-eutectic reaction L+$TiNi_2Sn$→ Ni_3Sn_4+TiNiSn will occur at 1168.8 K, much higher than 973 K. According to Ref. [32] and our findings, this peri-eutectic reaction must occur below 973 K. We confirmed this with annealed alloys B13, C15 and other alloys which reflected the phase equilibrium among L, $TiNi_2Sn$, Ni_3Sn_4 and TiNiSn. This again reveals the requirement for this work.

Whether the τ phase is a stable compound or not remains undefined. In this work, the τ phase was observed at 873 K (annealed for 100 d) and 973 K (annealed for 90 d), but disappeared at 508 K.

6 Conclusions

1) Isothermal sections of Ti−Ni−Sn ternary system at 508, 873 and 973 K are established.

2) Ternary compounds $TiNi_2Sn$ and TiNiSn are found to be stable at 508, 873 and 973 K, while Ti_2Ni_2Sn and $(Ti_{1-x-y}Ni_xSn_y)Ni_3$ are stable at 873 and 973 K. A new binary phase with composition of about $TiSn_4$ is detected at 508 K.

3) A peri-eutectic reaction L+$TiNi_2Sn$→Ni_3Sn_4+ TiNiSn at a certain temperature between 873 and 973 K is deduced.

References

[1] OTSUKA K, REN X. Physical metallurgy of Ti−Ni-based shape memory alloys [J]. Progress in Materials Science, 2005, 50(5): 511−678.

[2] ZHENG Y F, YANG F, MENG X L, CAI W, ZHAO L. Microstructure and phase transformation of TiNi alloy with addition of third element Sn [J]. Rare Metal Materials and Engineering, 2004, 33(6): 215−217.

[3] KIM J, IM Y M, NOH J, MIYAZAKI S, NAM T. Microstructures and martensitic transformation behavior of Ti−Ni−Sn alloys [J]. Scripta Materialia, 2011, 65(7): 608−610.

[4] CHOI H, KIM J, NOH J, MIYAZAKI J, KIM Y, NAM T. Crystallization behavior and microstructure of Ti−36Ni−7Sn (at.%) alloy ribbons [J]. Scripta Materialia, 2011, 65(7): 611−614.

[5] LU B C, XU J. Glass formation of Ti−Ni−Sn ternary alloys correlated with TiNi−Ti_3Sn pseudo binary eutectics [J]. Journal of Non-Crystalline Solids, 2008, 354(52): 5425−5431.

[6] JANG J, CHUN S, KIM N, CJO J, KIM J, YEOM J, KIM J, NAM T. Martensitic transformation behavior in Ti−Ni−X (Ag, In, Sn, Sb, Te, Tl, Pb, Bi) ternary alloys [J]. Materials Research Bulletin, 2013, 48(12): 5064−5069.

[7] CHOE H, KIM J, LEE S, NOH J, KIM Y, MIYAZAK S. Microstructure and martensitic transformation behavior of crystallized Ti−36Ni−7Sn (at%) alloy ribbons [J]. Journal of Alloys and Compounds, 2013, 577(S): s195−s199.

[8] MIYAZAK S, OTSUKA K. Deformation and transition behavior associated with the R-phase in Ti−Ni alloys [J]. Metallurgical and Materials Transactions A, 1986, 17(1): 53−63.

[9] SOEJIMA Y, MOTOMURA S, MITSUHARA M. In situ scanning electron microscopy study of the thermoelastic martensitic transformation in Ti−Ni shape memory alloy [J]. Acta Materialia, 2016, 103: 352−360.

[10] KAUFMAN L, NESOR H. Coupled phase diagrams and thermochemical data for transition metal binary systems—II [J]. CALPHAD, 1978, 2(1): 81−108.

[11] MURRAY J L. Phase diagrams of binary titanium alloys [M]. Metals Park, USA: ASM International, 1987: 197−211.

[12] LIANG H, JIN Z P. A reassessment of the Ti−Ni system [J].

CALPHAD, 1993, 17: 415−426.
[13] JIA C C, ISHIDA K, NISHIZAWA T. Experimental methods of phase diagram determination [M]. MORRAL J E, SCHIFFMAN R S, MERCHANT S M. The Mineral and Materials Society. Warrandale, USA, 1994: 31−38.
[14] BELLEN P, HARI KUMAR K C, WOLLANTS P. Thermodynamic assessment of the Ni−Ti phase diagram [J]. Zeitschrift für Metallkunde, 1996, 87(12): 972−978.
[15] TANG W, SUNDMAN B, SANDSTRÖM R, QIU C. New modelling of the B2 phase and its associated martensitic transformation in the Ti−Ni system [J]. Acta Materialia, 1999, 47(12): 3457−3468.
[16] DEKEYZER J, CACCIAMANI G, DUPIN N, WOLLANTS P. Thermodynamic modeling and optimization of the Fe−Ni−Ti system [J]. CALPHAD, 2009, 33(1): 109−123.
[17] TOKUNAGA T, HASHIMA K, OHTANI H, HASEBE M. Thermodynamic analysis of the Ni−Si−Ti system using thermochemical properties determined from Ab Initio calculations [J]. Materials transactions, 2004, 45(5): 1507−1514.
[18] SANTHY K, KUMAR K C H. Thermodynamic reassessment of Nb−Ni−Ti system with order–disorder model [J]. Journal of Alloys and Compounds, 2015, 619: 733−747.
[19] POVODEN-KARADENIZ E, CIRSTEA D C, LANG P, WOJCIK T. Thermodynamics of Ti−Ni shape memory alloys [J]. CALPHAD, 2013, 41: 128−139.
[20] FINLAY W L, JAFFEE R I, PARCEL R W, DURSTEIN R C. Tin increases strength of Ti−Al alloys without loss in fabricability [J]. J Metals, 1954: 6(1): 25−29.
[21] McQUILLAN A D. A study of the behaviour of titanium-righ alloys in the titanium-tin and titanium-aluminum systems [J]. J Inst Metals, 1955, 83: 181−184.
[22] GLAZOVA V V, KURNAKOV N N. Equilibrium in the titanium-tin system [J]. Doklady Akademii Nauk SSSR, 1960, 134(5): 1087−1090.
[23] BONDAR A A, VELIKANOVA T Y, BORYSOV D B, ARTYUKH L V, BILOUS O O, BURKA M P, FOMICHOV O S, TSYGANENKO N I, FIRSTOV S O. Titanium-boride eutectic materials: Phase equilibria and properties of alloys in the Ti-rich portion of the Ti−Sn−B system [J]. Journal of Alloys and Compounds, 2005, 400(1): 202−208.
[24] EREMENKO V N, VELIKANOVA T Y. Study of the tin-titanium system in the high-tin-content region [J]. Zhurnal Neorganicheskoi Khimii, 1962, 7(7): 1750−1752.
[25] KUPER C, WEIQUN P, PISCH A, GOESMANN F, SCHMID-FETZER R. Phase formation and reaction kinetics in the system Ti−Sn [J]. Zeitschrift für Metallkunde, 1998, 89(12): 855−862.
[26] YIN F, TEDENAC J C, GASCOIN F. Thermodynamic modeling of the Ti−Sn system and calculation of the Co−Ti−Sn system [J]. CALPHAD, 2007, 31(3): 370−379.
[27] NASH P, NASH A. The Ni−Sn (Nickel−Tin) system [J]. Journal of Phase Equilibria, 1985, 6(4): 350−359.
[28] GHOSH G. Thermodynamic modeling of the nickel-lead-tin system [J]. Metallurgical and Materials Transactions A, 1999, 30(6): 1481−1494.
[29] LIU H S, WANG J, JIN Z P. Thermodynamic optimization of the Ni−Sn binary system [J]. CALPHAD, 2004, 28(4): 363−370.
[30] STADNYK Y V, SKOLOZDRA R V. 770 K isothermal section of the Ti−Ni−Sn system [J]. Inorganic Materials, 1991, 27(10): 1884−1885.
[31] ROMAKA V V, ROGL P, ROMAKA L, STADNYK Y, MELNYCHEKO N, GRYSIV A, FALMBIGL M, SKRYABINA N. Phase equilibria, formation, crystal and electronic structure of ternary compounds in Ti−Ni−Sn and Ti−Ni−Sb ternary systems [J]. Journal of Solid State Chemistry, 2013, 197: 103−112.
[32] GÜRTH M, GRYTSIV A, VRESTAL J, ROMAKA V V, GIESTER G, BAUER E, ROGL P. On the constitution and thermodynamic modelling of the system Ti−Ni−Sn [J]. RSC Advances, 2015, 5(112): 92270−92291.
[33] SCHUSTER J C, NAKA M, SHIBAYANAGI T. Crystal structure of $CuSn_3Ti_5$ and related phases [J]. Journal of Alloys and Compounds, 2000, 305(1): L1−L3.
[34] BERCHE A, TÉDENAC J C, FARTUSHNAJ, JUND P. Calphad assessment of the Ni−Sn−Ti system [J]. CALPHAD, 2016, 54: 67−75.

Ti−Ni−Sn 三元系相平衡测定

王 檬，刘华山，蔡格梅，金展鹏

中南大学 材料科学与工程学院，长沙 410083

摘 要：采用平衡合金法，利用 X 射线衍射法(XRD)以及电子探针显微分析(EPMA)，研究了 Ti−Ni−Sn 三元系的平衡相组成及成分。结果表明，在 508 K 时，该体系中存在一个新的二元相 $TiSn_4$(摩尔分数，%)。此外，测定 $(Ti_{1-x-y}Ni_xSn_y)Ni_3$ 相 (τ, $AuCu_3$-type) 在 873 和 973 K 稳定存在。根据不同退火样品的显微组织，在 Ti−Ni−Sn 三元系中检测到 4 个三元相：TiNiSn、$TiNi_2Sn$、Ti_2Ni_2Sn 和 $(Ti_{1-x-y}Ni_xSn_y)Ni_3$。构建 Ti−Ni−Sn 三元系在 508、873 和 973 K 的等温截面。通过对比 3 个等温截面，在 873~973 K 发生包共晶反应：$L+TiNi_2Sn \rightarrow Ni_3Sn_4+TiNiSn$。并测定了 Sn 在 TiNi 和 Ni 在 Ti_5Sn_3 中的固溶度。

关键词：等温截面；Ti−Ni−Sn 系；相平衡

(Edited by Bing YANG)